Ab Initio Calculations on Normal Mode Vibrations and the Raman and IR Spectra of the $[B_3O_6]^{3-}$ Metaborate Ring

Kechen Wu[†] **and Soo-Y. Lee***[,‡]

Departments of Computational Science and Chemistry, National University of Singapore, Kent Ridge, Singapore 119260, Singapore

Received: August 7, 1996; In Final Form: October 30, 1996[⊗]

Normal vibrational modes of the $[B_3O_6]^{3-}$ metaborate ring are obtained at the Hartree−Fock level by *ab initio* calculations. The Raman and IR spectra are predicted, and the former are compared with available experimental results of molten crystal metaborates that contain $[B_3O_6]^{3-}$ rings, i.e., β-BaB_2O_4 and $CsBO_2$ crystals. The internal vibrations of the $[B_3O_6]^{3-}$ ring are dominant in the whole crystal lattice vibrations of these nonlinear optical crystals. Also, the $[B_3O_6]^{3-}$ ring accounts for the IR transparency cut-off in such crystals. It is deduced from the predicted IR spectrum of a $[B_3O_6]^{3-}$ ring that the transparency cut-off frequency of the β-BaB_2O_4 crystal on the IR side is below 4000 cm^{-1} (>2.5 μm), which agrees well with the measured data. This study is also useful for understanding the vibrational contributions to nonlinear optical polarizabilities.

1. Introduction

Theoretical calculations on nonlinear optical (NLO) polarizabilities are an intensely active field because they are directly related to the design of novel NLO materials at the molecular level.[1,2] The linear and nonlinear polarizabilities are expressed by the wave functions of electrons and nuclei. Invoking the Born−Oppenheimer approximation, the contributions of electrons and nuclei are calculated separately. Most of the efforts have been focused on the electronic contributions.[3] However, recent studies[4−10] have pointed out that it is not always the case that the vibrational contributions are negligible, especially for observables in the IR range. The coupling between the electronic and nuclear motions may result in electronic delocalization, and hence, vibrations can make contributions to the optical polarizability. In fact, in some cases, the vibrational contribution is dominant compared with its electronic counterpart. Bishop and Kirtman have developed a method,[11,12] the BK method, for calculating dynamic vibrational polarizability. This method depends on the accurate analysis of the normal mode vibrations.

Another possible contribution of the normal mode vibrations is to the transparency cut-off on the IR side of the NLO materials. As we know, the transparency range is one of the most important parameters of a NLO material in device applications. According to the studies of Wu and Chen,[13] the electronic transitions contribute to the transparency cut-off on the UV side of most of the NLO materials. In this paper, we demonstrate that the transparency cut-off on the IR side of the β-BaB_2O_4 crystal is mainly determined by the vibrational transitions between the vibrational levels of the constituent NLO-active groups, the $[B_3O_6]^{3-}$ rings. This may be the first time that the transparency range of the NLO materials is estimated theoretically.

In this paper, we take the barium metaborate crystal, β-BaB_2O_4 (BBO), as an example to demonstrate the calculation of the normal mode vibrations of NLO materials. The BBO crystal is well suited for this theoretical treatment because several experimental studies have been made on its vibrational spectra.[14−17] Not all the known NLO materials, however, have measured vibrational information available, but the theoretical approach here is relevant to them. In practice, it is difficult to calculate the vibrational property, e.g., IR spectrum, of a material. A possible approach for a NLO material is to divide the unit cell into independent bonds or molecular groups and express the nuclei contribution in terms of the normal mode vibrations of these entities, neglecting the overlap or any ground-state interaction between these groups. Using this approach, the study of normal mode vibrations of a BBO crystal is reduced to the study of its structural units: $[B_3O_6]^{3-}$ anionic group and Ba^{2+} cation.[18] Ba^{2+} is a heavy ion, and therfore, its vibrational contribution is in the *far*-IR range. If we confine our discussion to the IR range, we can focus our study on the normal mode vibrations of the $[B_3O_6]^{3-}$ metaborate ring.

Previous theoretical studies of the vibrations of the $[B_3O_6]^{3-}$ unit were based on a force-field calculation to fit the measured frequencies.[16] However, in this paper, *ab initio* methods are adopted to investigate the normal modes and frequencies of the $[B_3O_6]^{3-}$ metaborate ring. The Raman and IR spectra are also calculated. The former has been compared with experimental results, and the latter can be used to predict the transparency cut-off on the IR side. The computational details are given in section 2, while the results and discussion are presented in section 3.

2. Computational Details

Ab initio calculations at the RHF/6-31+g(d,p) level were performed on a Cray J916 supercomputer with the Gaussian-94 package.[19] A double-ζ-valence (DZV) basis set 6-31+g-(d,p) was used in all the calculations with a total of 171 basis functions. Diffusive functions in the basis set were used to account for the $[B_3O_6]^{3-}$ ring being negatively charged. The optimized equilibrium structure was determined by the simultaneous relaxation of all the geometric parameters (bond lengths, bond angles, and dihedral angles) to obtain the energy minimum, where a tight convergence threshold was utilized. Vibrational frequencies were calculated by the second derivatives of the total energy with respect to atomic displacements about the equilibrium geometry. Raw vibrational frequencies computed at the Hartree−Fock level contain known systematic overesti-

[†] Department of Computational Science.
[‡] Department of Chemistry.
[⊗] Abstract published in *Advance ACS Abstracts,* January 1, 1997.

S1089-5639(96)02388-2 CCC: $14.00

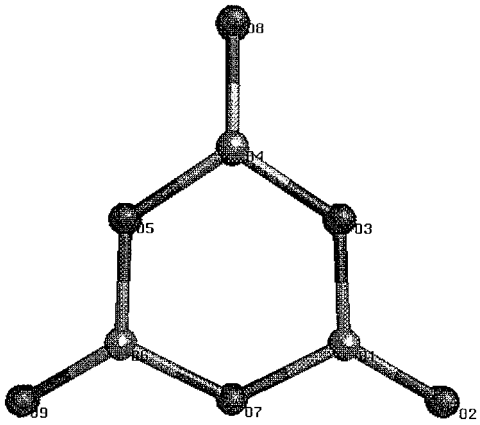

Figure 1. Optimized structure of the $[B_3O_6]^{3-}$ metaborate ring.

TABLE 1: Optimized Structure Parameters and Energy[a] for the $[B_3O_6]^{3-}$ Unit

Parameter	RHF/6-31G+(d,p)
$r(B_1-O_2)$	1.314 3
$r(B_1-O_3)$	1.416 5
$r(B_1-O_7)$	1.416 5
$\angle O_2-B_1-O_3$	123.1 496
$\angle O_3-B_1-O_7$	113.7 041
$\angle B_1-O_7-B_6$	126.2 959
$-(E+523)$	0.359 831

[a] Bond lengths in Å, bond angles in degrees, and energy in hartrees.

mations of about 10−12% due to the neglect of the electron correlation. Our calculated vibrational wavenumbers were thus scaled by a factor of 0.9 before being compared with experimental results. The quantitative vibrational displacement configurations of the $[B_3O_6]^{3-}$ metaborate ring were analyzed with *Unichem* software.[20]

The Raman scattering cross sections, $\partial\sigma_j/\partial\Omega$, which are proportional to the Raman intensities, were calculated from the Raman scattering activities and the predicted wavenumbers for each normal mode using the expression[21]

$$\frac{\partial\sigma_j}{\partial\Omega} = \left(\frac{2\pi^2}{45}\right)\left[\frac{(\nu_0-\nu_j)^4}{1-e^{-hc\nu_j/kT}}\right]\left(\frac{h}{c\nu_j}\right)S_j$$

where ν_0 is the excitation wavenumber. The calculated Raman spectrum used $\nu_0 = 19\,600$ cm^{-1} (510.5 nm) to correspond to the observed Raman spectra taken with an argon ion laser.[16] The vibrational wavenumber of the *j*th normal mode is denoted by ν_j; S_j is the corresponding calculated Raman scattering activities. The Raman scattering cross sections, IR intensities, and vibrational frequencies were used together with a Lorentzian function to obtain the calculated Raman and IR spectra for comparison with experiments.

3. Results and Discussion

The optimized structure of a $[B_3O_6]^{3-}$ ring has D_{3h} point group symmetry, which is shown in Figure 1. The ring is a slightly distorted hexagon but planar (the angle of BOB is slightly larger than for OBO; the ring B−O bond is longer than the side B−O bond). The structural parameters are summarized in Table 1. The total vibrational representation is as follows:

$$\Gamma = 3A'_1 + 2A'_2 + 5E' + 2A''_2 + 2E''$$

All the 21 normal modes are illustrated in Figure 2, where each arrow length gives the relative calculated vibrational displacement of the corresponding atom.

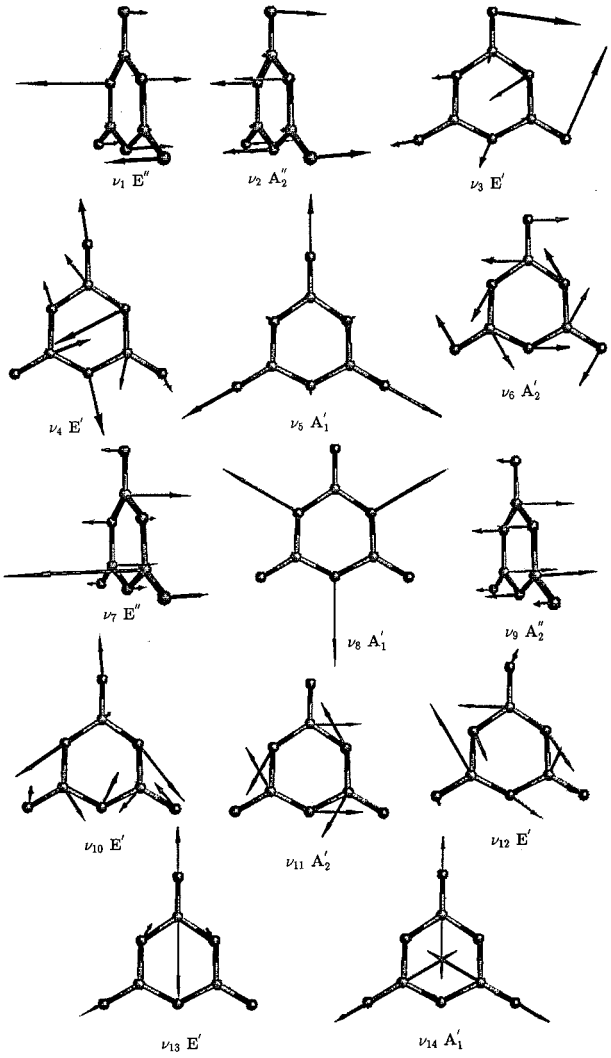

Figure 2. Calculated normal mode vibration of the $[B_3O_6]^{3-}$ metaborate ring. The relative length of each arrow denotes the vibrational displacement.

Ten normal modes are Raman active, $2E'' + 5E' + 3A'_1$. The calculated Raman spectrum of a $[B_3O_6]^{3-}$ metaborate ring is shown in Figure 3c and is compared with both the high-temperature (Figure 3b) and ambient experimental Raman spectra (Figure 3a) of the BBO crystal. It is known that the Raman spectrum of the molten BBO crystal (at 1190 K) shows the characteristics of the internal vibrations of the structural units, $[B_3O_6]^{3-}$ rings in this case. The results of the calculated vibrational frequencies of the $[B_3O_6]^{3-}$ ring and the experimental results for molten BBO and $CsBO_2$ (CBO, whose structural units are also $[B_3O_6]^{3-}$ rings) are shown in Table 2. The general agreement of the calculated and experimental results indicates the reliability of the theoretical calculations.

There are some minor differences between the calculated Raman spectrum of the $[B_3O_6]^{3-}$ ring and the observed molten crystal spectra. We predict a low-frequency Raman mode (ν_1, 95 cm^{-1}) of medium intensity, which requires FT Raman spectroscopy for its measurement. A weak-to-medium Raman peak of A_1 symmetry at 540 cm^{-1}, as a shoulder to ν_5 on the low-frequency side, was observed in the molten spectra but is not found in the calculation. This mode is believed to be due to the totally symmetric *external* vibrations among the $[B_3O_6]^{3-}$ rings in the crystal, which is out of the range of our internal vibration calculation. The calculated weak Raman peak of mode ν_{12} at 1140 cm^{-1} is barely observable in the crystal spectrum in Figure 3a. On heating, two Raman peaks appear in the range

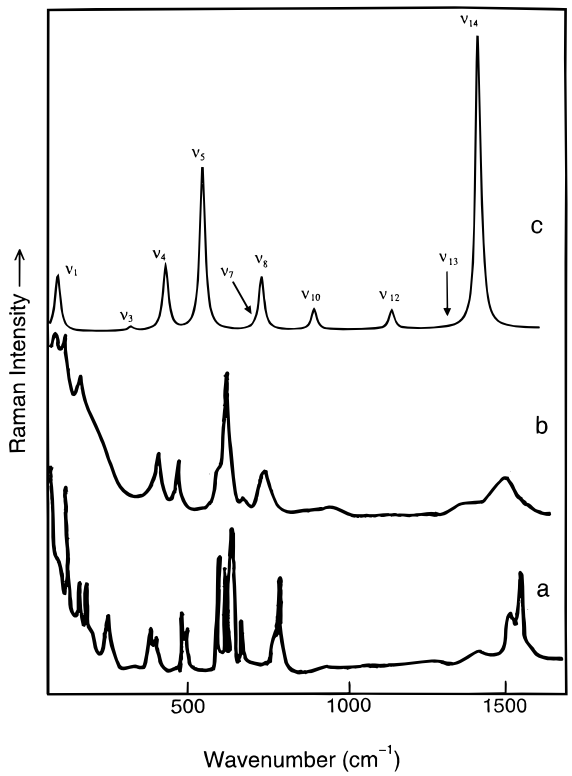

Figure 3. Calculated Raman spectrum of the $[B_3O_6]^{3-}$ metaborate ring, compared with the experimental results of Voronko *et al.*[16]: Unpolarized Raman spectrum of (a) the β-BaB_2O_4 single crystal and (b) a crystallized BaB_2O_4 melt at 1150K. (In the calculated curve, ν_7 and ν_{13} are too weak to be seen.)

TABLE 2: Calculated Raman Frequencies for the $[B_3O_6]^{3-}$ Unit and Observed for the BBO and CBO Crystals

vib	*ab initio*[a]	fix scaled[b]	Raman cross sect[c]	obs[d] BBO	obs[d] CBO	approx description
ν_1	106E″	95.5E″	2.13			out-of-plane bend
ν_3	361E′	324E′	0.15	400E, m	380E, m	B−O−B bend
ν_4	481E′	432E′	1.00	476E, m	462E, m	O−B−O bend
				540A_1, m	544A_1, m	
ν_5	608A_1′	547A_1′	6.20	630A_1, s	606A_1, s	B−O sym. stretch
ν_7	789E″	710E″	0.09	710E, w	713E, w	out-of-plane bend
ν_8	814A_1′	733A_1′	2.02	751A_1, m	747A_1, m	B−O−B bend
ν_{10}	996E′	896E′	0.79	939E, w	930E, w	B−O asym. stretch
ν_{12}	1267E′	1140E′	0.73			B−O asym. stretch
ν_{13}	1476E′	1328E′	0.0001	1389E, w	1390E, w	B−O asym. stretch
ν_{14}	1570A_1′	1413A_1′	11.20	1460A_1, s	1503A_1, s	B−O sym. stretch

[a] Calculated using RHF/6-31+g(d,p). [b] Calculated using scaling factor of 0.9. [c] Calculated unpolarized Raman scattering sections ($\times 10^{-8}$ m^2). [d] BBO melt at 1190 K and CBO melt at 1055 K.

of 1000−1250 cm^{-1} with increasing intensities as the temperature rises above the melting point in the experiments (see Figure 3b and c in ref 16). Voronko *et al.*[16] assigned these modes to the Raman lines of the broken $[B_3O_6]^{3-}$ ring, which cannot be determined in our calculations. The predicted Raman peak of ν_{13} at 1328 cm^{-1} is very weak, but there is a stronger peak at 1389 cm^{-1} in the measured spectrum. This could be due to the intensity of the measured peak of ν_{13} (1329 cm^{-1}) being strengthened through the combination of measured ν_4 (432 cm^{-1}) and ν_{10} (896 cm^{-1}), which is located at about the same frequency.

It is not surprising to see that the ambient Raman spectrum of the BBO crystal is clearly characterized by the Raman spectrum of the $[B_3O_6]^{3-}$ ring (see Figure 3), which means that the internal vibrations of the $[B_3O_6]^{3-}$ ring play a dominant role in the whole crystal lattice vibrations. Peak splittings occur in

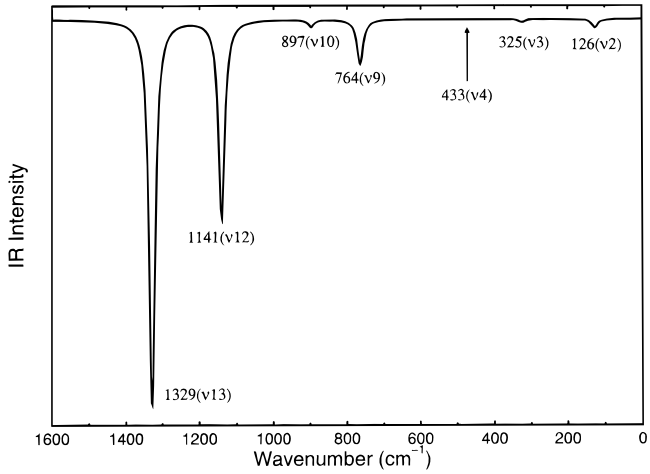

Figure 4. Calculated IR spectrum of the $[B_3O_6]^{3-}$ metaborate ring.

the crystal spectrum. These splittings can be attributed to the correlation effect in the crystal which may reduce the symmetry of some of the vibrational modes. For example, the strong ν_5 mode at about 600 cm^{-1} which is due to the symmetrical stretch of boron and outer oxygens (see Figure 2) splits into many lower symmetry modes in the crystal spectrum because of the correlation effect in the crystal. A difference is also found in the relative intensity of ν_{14}. There are two reasons for the discrepancy: ν_{14} is due to the symmetric stretch of boron and oxygens, and this mode is restrained by the crystal field effect; the other reason comes from our experience that it is usually difficult to accurately measure the relative Raman intensity in the short-wavelength region.

The IR-active modes consist of 2A″ + 5E″ (ν_2, ν_3, ν_4, ν_9, ν_{10}, ν_{12}, and ν_{13}). The calculated IR spectrum is shown in Figure 4. The highest IR-active frequency lying at 1329 cm^{-1}, which is relevant to the absorption cut-off on the IR side, has a very strong IR intensity (*ab initio* result of 1710 kM/mol). Consequently, the first and second *overtones* of this fundamental line, corresponding to the vibrational transitions from the ground state to the second and third excited states, at 2658 and 3987 cm^{-1}, respectively, will be strong enough to make contributions to the IR absorption of the BBO crystal. Typically, the intensity of the first overtone line is about 20% that of the fundamental line, and the intensity of the second overtone line is again 20% that of the first one, and so on. Thus, the third overtone intensity at 5316 cm^{-1} (1.88 μm) is predicted to be less than 14 kM/mol, which is almost undetectable. This means that the transparency cut-off on the IR side of the BBO crystal is at the second overtone line at 3987 cm^{-1} (2.51 μm), which agrees well with the measured result of 2.6 μm.[22]

4. Conclusion

Ab initio calculations have been made on the normal mode vibrations of the $[B_3O_6]^{3-}$ metaborate ring. The assignments of the normal modes were presented in detail. The theoretical results for the Raman spectrum compared well with experiments. It has already been shown that the $[B_3O_6]^{3-}$ metaborate ring is the origin of some NLO properties of the BBO crystal, like the NLO susceptibilities in the UV and visible range,[22] the absorption cut-off on the UV side,[13] and birefringence.[23] This study reveals that the $[B_3O_6]^{3-}$ ring again plays a key role in the vibrational properties of the BBO and CBO crystals. The calculated IR spectrum is obtained, but no experimental data are currently available for comparison. We estimated the transparency cut-off on the IR side of such crystals from the calculated IR spectrum. More studies on other NLO materials

about their transparency cut-off on the IR side are in progress. The theoretical predictions in this paper are sufficiently reliable, and the method can be extended to the normal mode vibration studies of other NLO materials where the anionic groups or molecules govern the vibrational spectra. It also provides a foundation for theoretical studies on the nuclei contributions to the NLO susceptibility of the materials.

Acknowledgment. K. Wu acknowledges the financial support from the National Science and Technology Board of Singapore. We thank Mr. Z. W. Feng for his technical assistance.

References and Notes

(1) Shelton, D. P.; Rice, J. E. *Chem. Rev.* **1994**, *94*, 3.

(2) Ratner, M. A. *Int. J. Quant. Chem. Special Issue Molec. Nonlinear Opt.* **1992**, 43.

(3) See, for example: Nobutoki, H.; Koezuk, H. *J. Phys. Chem.* **1996**, *16*, 645.

(4) Papodopoulos, M. G.; Willetts, A.; Handy, N. C.; Underhill, A. E. *Mol. Phys.* **1996**, *88*, 1063.

(5) Kirtman, B.; Champagne, B.; André, J. *J. Chem. Phys.* **1996**, *104*, 4125.

(6) Champagne, B.; Perpète, E.; André, J. *J. Chem. Soc., Faraday Trans.* **1995**, *91*, 1641.

(7) Champagne, B.; Perpète, E.; André, J. *J. Chem. Phys.* **1994**, *101*, 10796.

(8) Cohen, M. J.; Willets, A.; Amos, R. D.; Handy, N. C. *J. Chem. Phys.* **1994**, *100*, 4467.

(9) Bishop, D. M.; Kirtman, B.; Kurtz, H. A.; Rice, J. E. *J. Chem. Phys.* **1993**, *98*, 8024.

(10) Bishop, D. M.; Kirtman, B. *J. Chem. Phys.* **1991**, *95*, 2646.

(11) Kirtman, B.; Bishop, D. M. *Chem. Phys. Lett.* **1990**, *175*, 601.

(12) Bishop, D. M.; Kirtman, B. *J. Chem. Phys.* **1992**, *97*, 5255.

(13) Wu, K.; Chen, C. *Appl. Phys.* **1992**, *A54*, 209.

(14) Lai, X.; Wu, G. *Spectrochim. Acta* **1987**, *43A*, 1421.

(15) Lu, J.; Lan, G.; Li, B.; Yang, Y.; Wang, H.; Wu, B. *J. Phy. Chem. Solids* **1988**, *49*, 519.

(16) Voronko, Y. K.; Gorbachev, A. V.; Osiko, V. V.; Sobol, A. A.; Feigelson, R. S.; Route, R. K. *J. Phys. Chem. Solids* **1993**, *54*, 1579.

(17) Hong, S.; Wu, B. *Chin. Phys. Lett.* **1995**, *12*, 366.

(18) Frohlich, R. *Z. Kristall.* **1984**, *168*, 109.

(19) Gaussian 94, Revision B.3, Frisch, M. J.; Trucks, G. W.; Schlegel, H. B.; Gill, P. M. W.; Johnson, B. G.; Robb, M. A.; Cheeseman, J. R.; Keith, T.; Petersson, G. A.; Montgomery, J. A.; Raghavachari, K.; Al-Laham, M. A.; Zakrzewski, V. G.; Ortiz, J. V.; Foresman, J. B.; Peng, C. Y.; Ayala, P. Y.; Chen, W.; Wong, M. W.; Andres, J. L.; Replogle, E. S.; Gomperts, R.; Martin, R. L.; Fox, D. J.; Binkley, J. S.; Defrees, D. J.; Baker, J.; Stewart, J. P.; Head-Gordon, M.; Gonzalez, C.; Pople, J. A. Gaussian, Inc., Pittsburgh, PA, 1995.

(20) Unichem 3.0, Cray Research, Inc., 1995.

(21) Chantry, G. W. In *The Raman Effect*; Anderson, A., Ed.; Marcel Dekker: New York, 1971; Vol. 1, Chapter.2.

(22) Kato, K. *IEEE J. Quantum Elect.* **1986**, *22*, 1013.

(23) Wu, K.; Chen, C. *Chem. Phys. Lett.* **1992**, *196*, 62.